



# Heavy scalar searches in the $t\bar{t}$ channel at the LHC (theory)

Zhen Liu (Fermilab)

LHC Dark Matter WG public meeting

Dec. 15<sup>th</sup>, 2016

Based on work M. Carena, ZL, [arXiv:1608.07282](https://arxiv.org/abs/1608.07282), JHEP

# Motivation

As you heard in the previous few talks, a completion of the (pseudo-)scalar mediator Dark Matter model is needed



The scalar mediator couple to fermions hierarchically, likely to decay dominantly to  $t\bar{t}$  or DM pairs



**$gg \rightarrow S \rightarrow t\bar{t}$  is an important channel for heavy scalar discovery and identification**

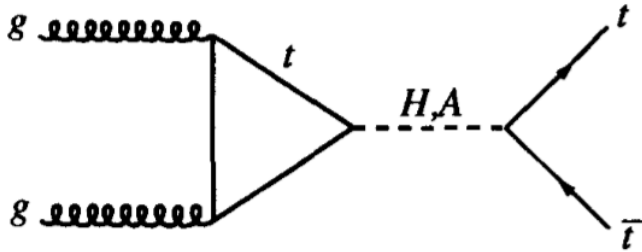


This channel is **challenging** in some *interesting* way and we try to seek for physics opportunities through this challenge

$$\mathcal{L}^{\text{Yukawa}} \supset \frac{y_i^s}{\sqrt{2}} \bar{t}tS + i \frac{\tilde{y}_i^s}{\sqrt{2}} \bar{t}\gamma_5 tS$$

$$\mathcal{L}^{\text{Yukawa}} \xrightarrow[\text{“effectively”}]{\text{loop-induced}} -\frac{1}{4} g_{Sgg}(\hat{s}) G_{\mu\nu} G^{\mu\nu} S - \frac{i}{2} \tilde{g}_{Sgg}(\hat{s}) \tilde{G}_{\mu\nu} G^{\mu\nu} S,$$

# Challenges (interferences)



$$\frac{\hat{s}}{(\hat{s} - m_S^2) + i\Gamma_S m_S} \approx \frac{m_S}{\Gamma_S} \frac{2\Delta - i}{4\Delta^2 + 1}$$

$$\text{with } \Delta \equiv \frac{\hat{s} - m_S^2}{2m_S\Gamma_S} \approx \frac{\sqrt{\hat{s}} - m_S}{\Gamma_S} \text{ for } \frac{\hat{s}}{m_S^2} - 1 \ll 1.$$

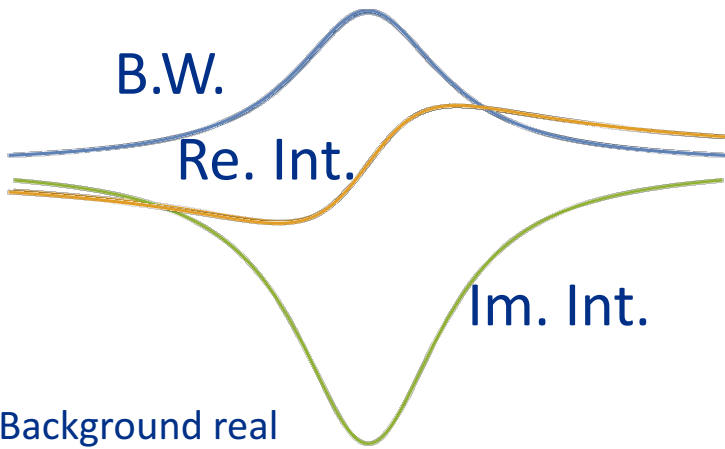
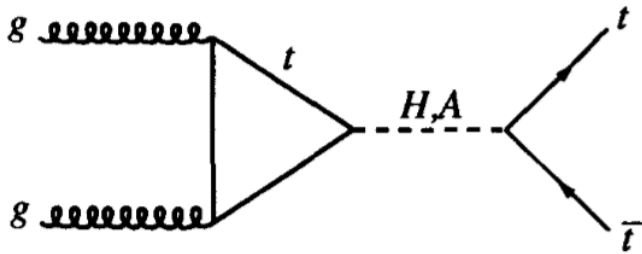
Background real

Re. Int.– Interference from the real part of the propagator

(normal interference, parton level no contribution to the rate, shift the mass peak)

(When convoluting with PDF, may generate residual contribution to signal rate;  
conventional wisdom, interference only important when width is large)

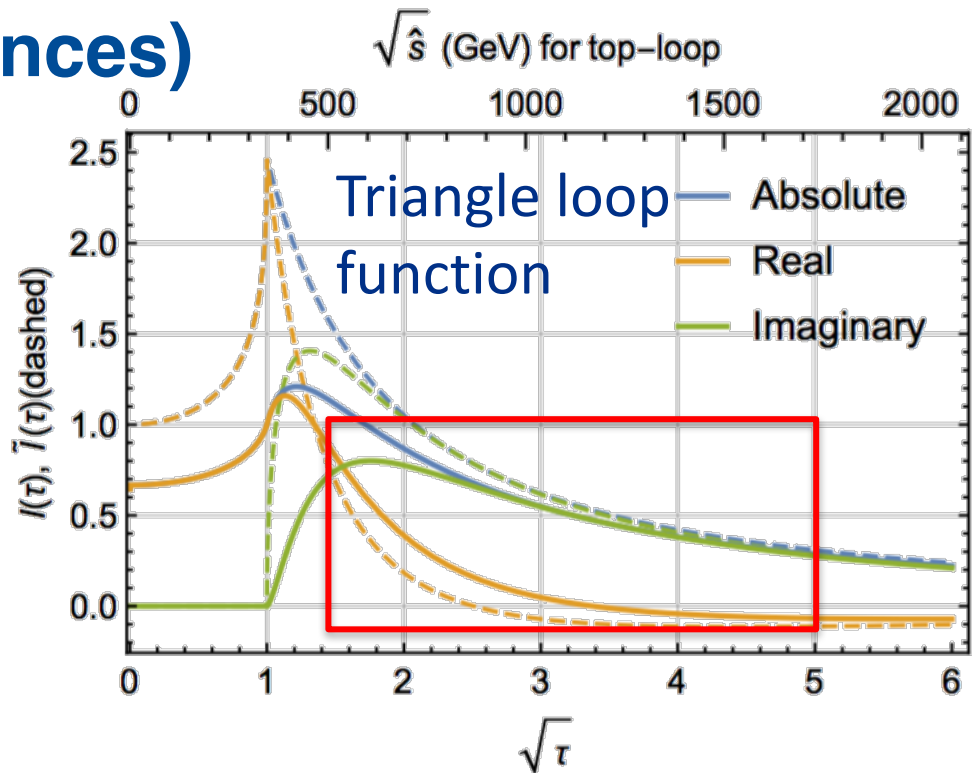
# Challenges (interferences)



Background real

Re. Int.– Interference from the real part of the propagator (normal interference, parton level no contribution to the rate, shift the mass peak)

Im. Int.– Interference from the imaginary part of propagator (rare case, changes signal rate)

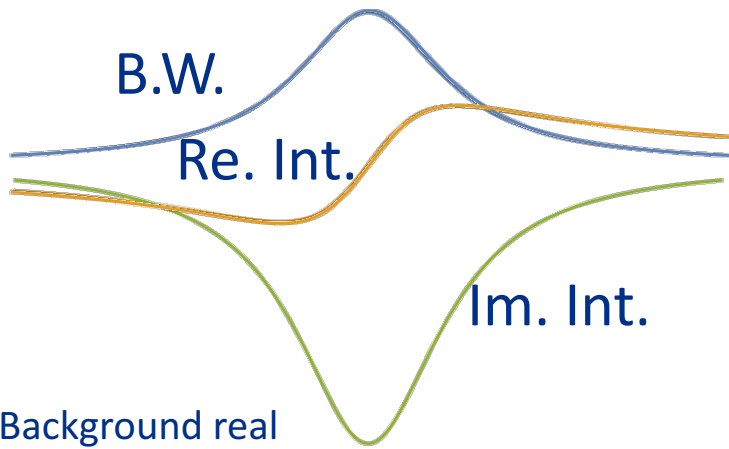
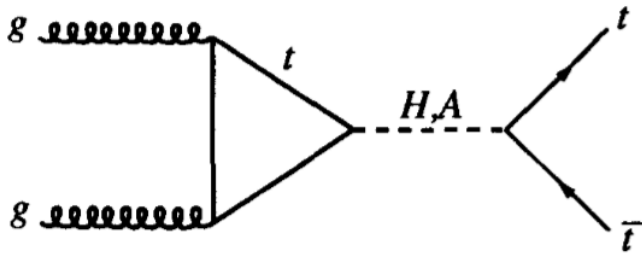


Once across the threshold, imaginary piece arises drastically and the real piece decreases.

A strong phase  
 “insensitive”\* to phase in the Yukawa as the signal amplitudes is proportional to  $|y_t|^2$ .

\*subject to difference in loop functions

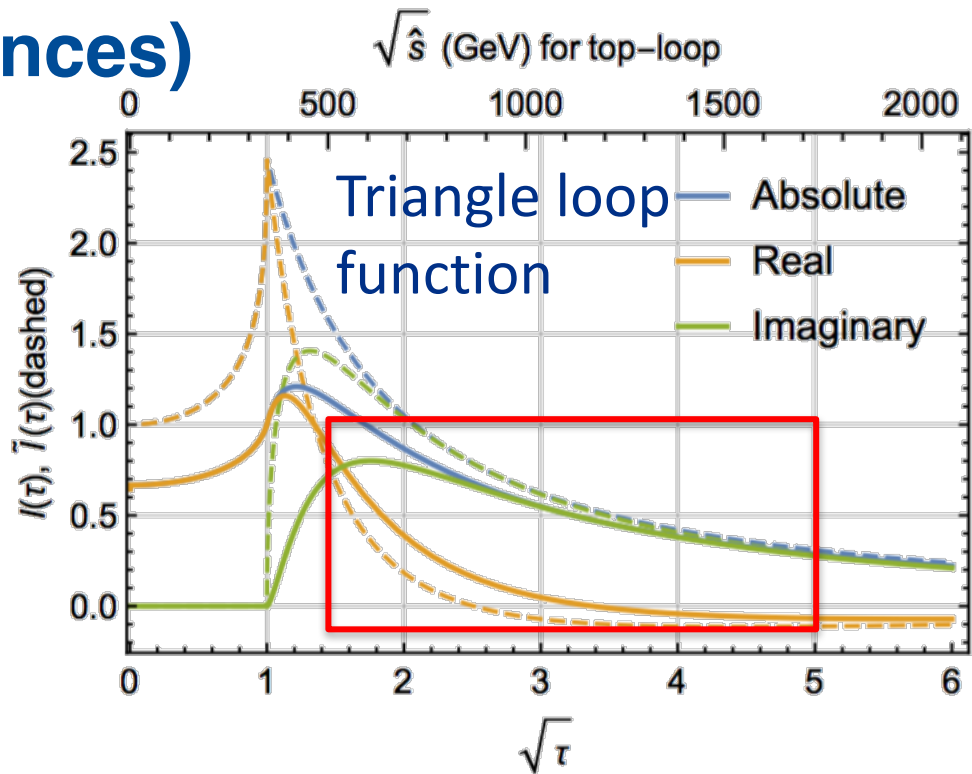
# Challenges (interferences)



Background real

Re. Int.– Interference from the real part of the propagator (normal interference, parton level no contribution to the rate, shift the mass peak)

Im. Int.– Interference from the imaginary part of propagator (rare case, changes signal rate)

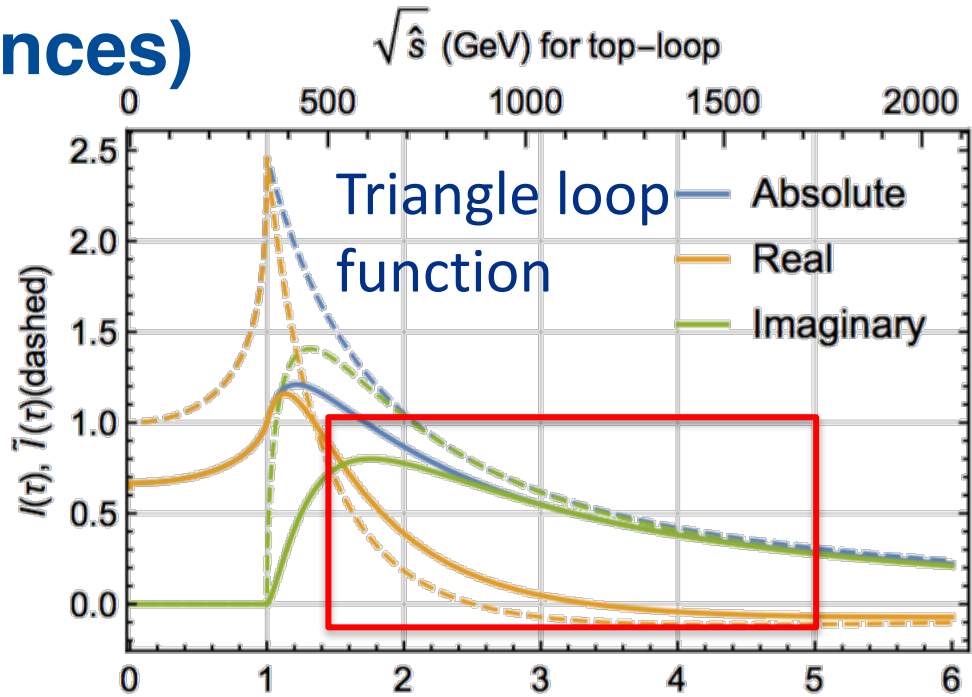
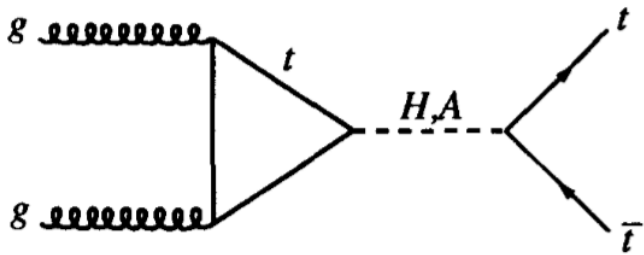


Once across the threshold, imaginary piece arises drastically and the real piece decreases.

A strong phase  
 “insensitive”\* to phase in the Yukawa as the signal amplitudes is proportional to  $|y_t|^2$ .

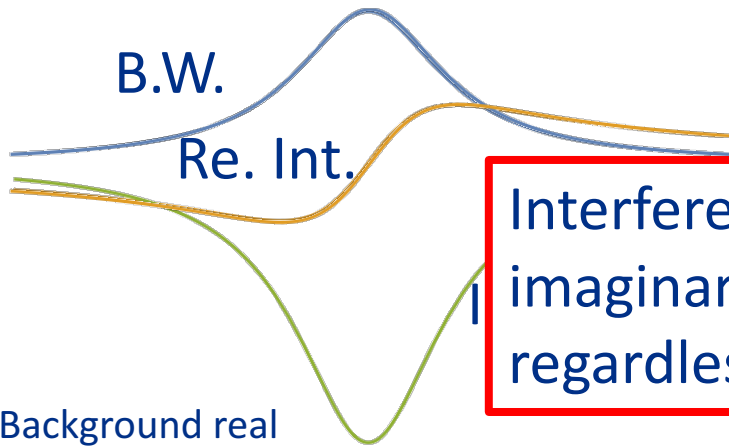
\*subject to difference in loop functions

# Challenges (interferences)



Interference effect from this imaginary part is important, regardless of the width!

threshold, imaginary piece and the real piece



Background real

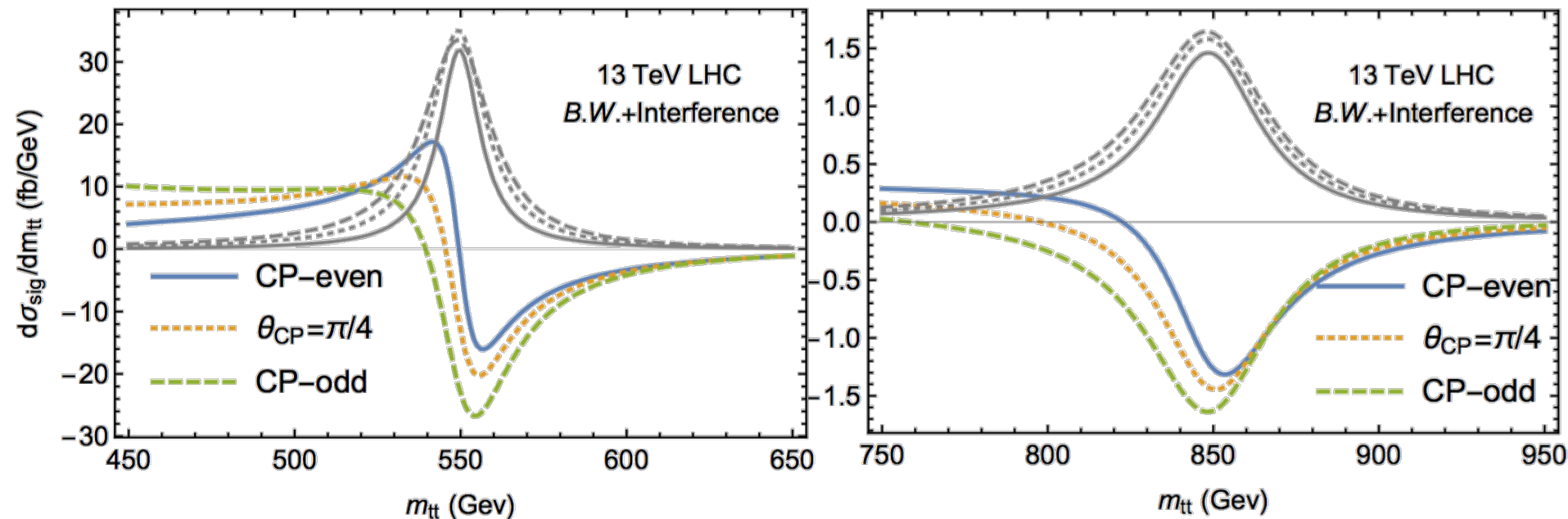
Re. Int.– Interference from the real part of the propagator (normal interference, parton level no contribution to the rate, shift the mass peak)

Im. Int.– Interference from the imaginary part of propagator (rare case, changes signal rate)

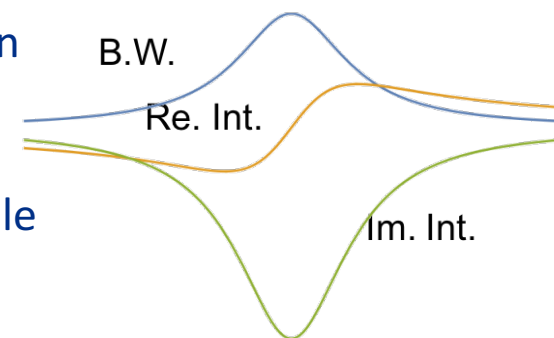
A strong phase “insensitive”\* to phase in the Yukawa as the signal amplitudes is proportional to  $|y_t|^2$ .

\*subject to difference in loop functions

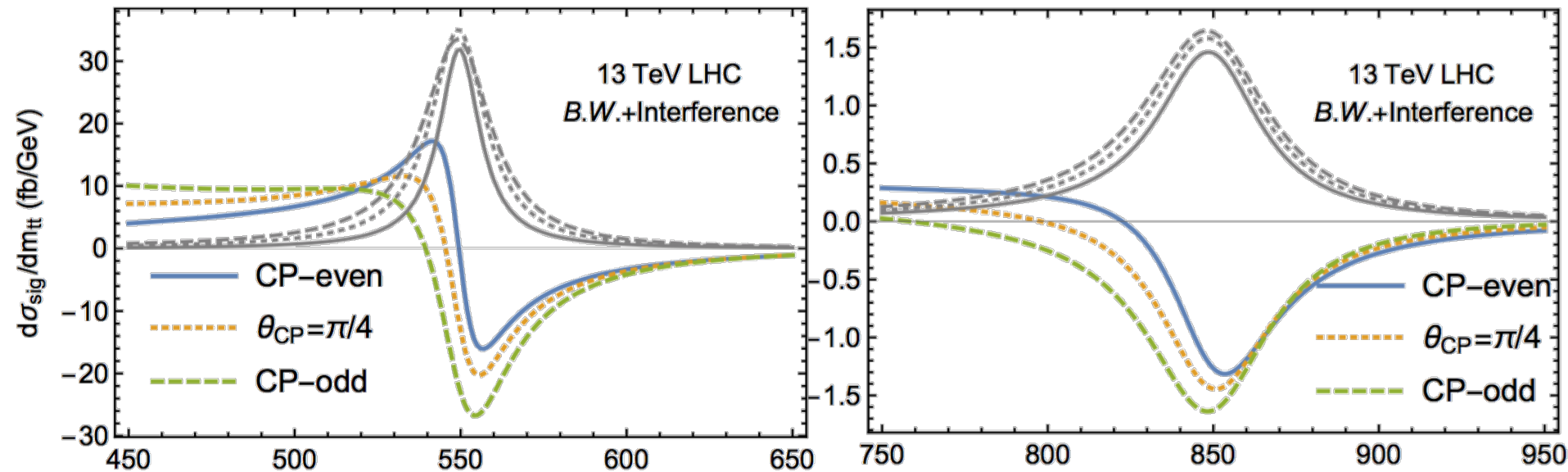
# Challenges



- Gray lines, Breit-Wigner contribution (subtle differences between the scalar case the pseudoscalar case);
- Colored lines, total BSM signal lineshapes;
- (Left panel) for 550 GeV scalars, the loop function has comparable real and imaginary components. The imaginary interference “cancels” the Breit-Wigner, leaving only Bump-dip structure;
- (Right panel) for 850 GeV scalar, the loop function is almost purely imaginary and the total lineshapes become a pure dip.



# Challenges



Special line shapes:

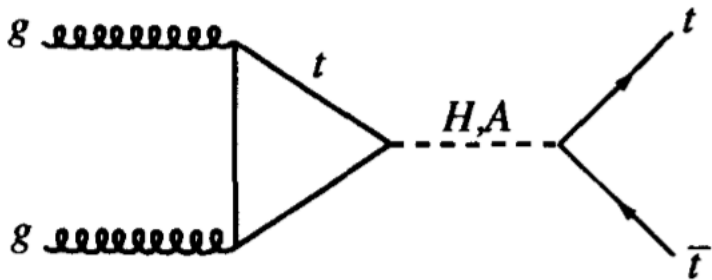
- a) Bump search not designed/optimized for this, have to modify our current search;
- b) Smearing effects erode the structure, making this signal much harder.

“cancels” the Breit-Wigner, leaving only Bump-dip structure;

- (Right panel) for 850 GeV scalar, the loop function is almost purely imaginary and the total lineshapes become a pure dip.



# Opportunities



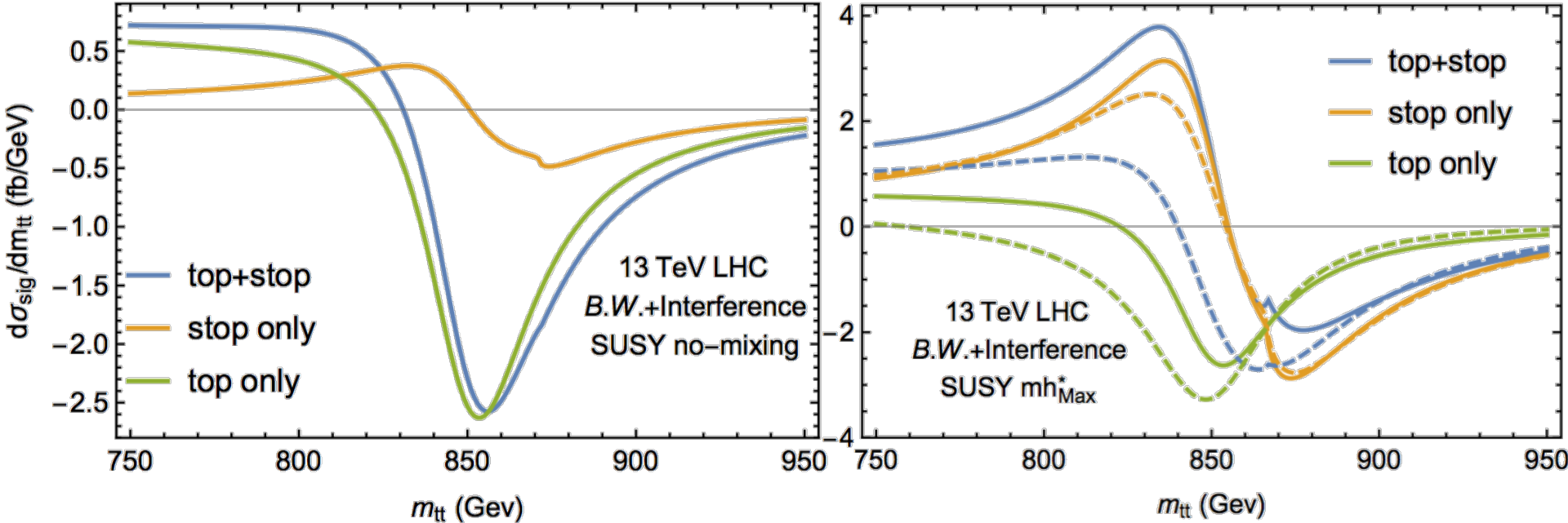
- Nearly degenerate CP-even and CP-odd scalars
- CP phases (new interferences emerges proportional to the loop-function difference between the even and odd one for nearly degenerate ones)

- Bottom-quark contributions (large  $\tan\beta$ , changes the relative phase)

- New colored particle contributions and threshold effects (stops, VLQs, etc., reduce the relative phases and recovers the bump search)

- New channels (associated production with top(s), bottoms, jet(s), etc. Potentially reducing the interference effect.)

# Opportunities– Stop contributions



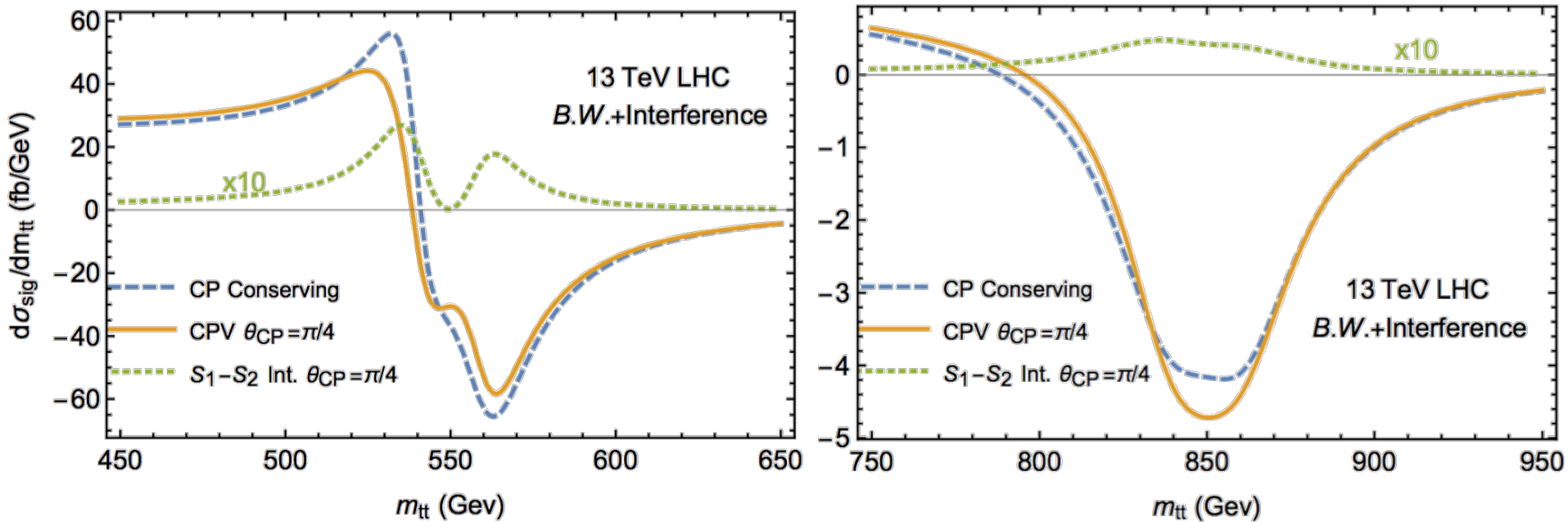
SUSY TeV scale stop quarks are highly anticipated through naturalness argument; Green curves are top contribution only, orange curves are stop contribution only and blue curves are with both top and stop contributions.

For 850 GeV scalars, we show two benchmark scenarios:

Stop zero L-R mixing, the stop contribution is only a small perturbation;

Stop large L-R mixing,  $mh_{\text{max}}^*$  scenario, the heavy Higgs to stop quark pair coupling is dominated by the mixing term, and significant changes could occur.

# Opportunities—nearly degenerate with CPV



(left panel) 540 and 560 GeV scalars

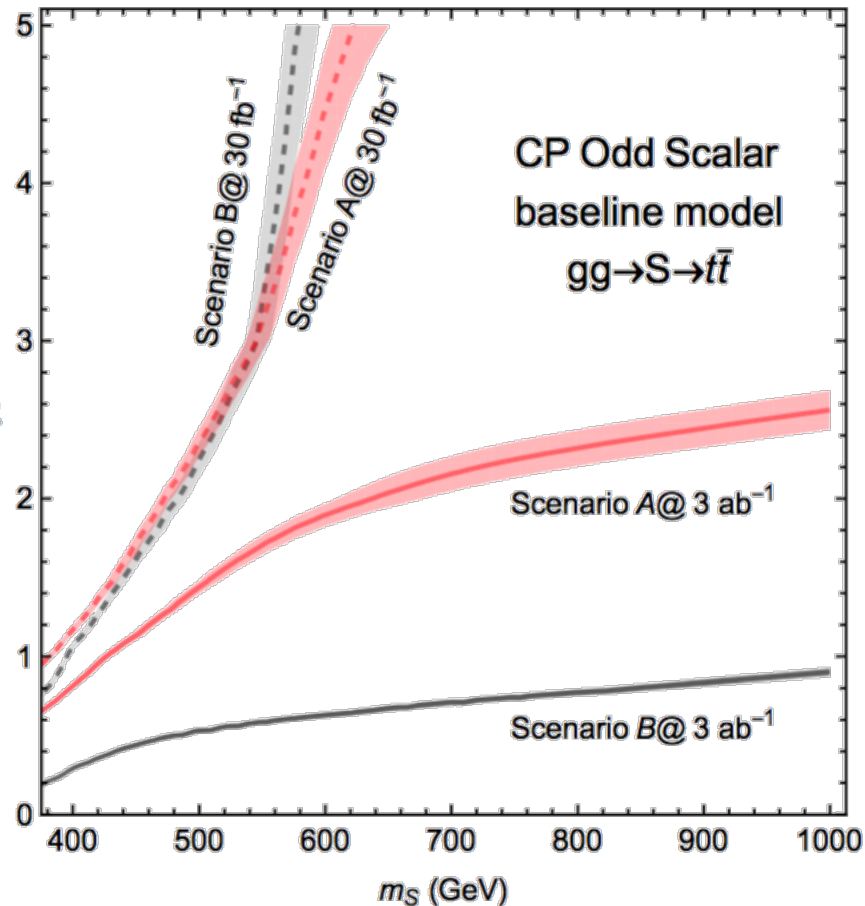
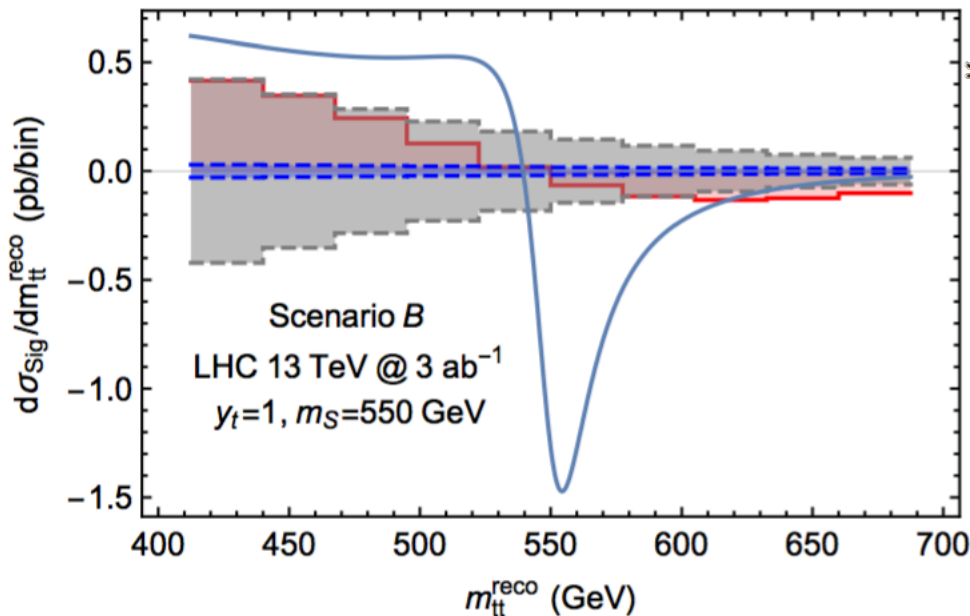
(right panel) 840 and 860 GeV scalars

The signature—bumps and dips—roughly doubled, increasing the potential sensitivity;

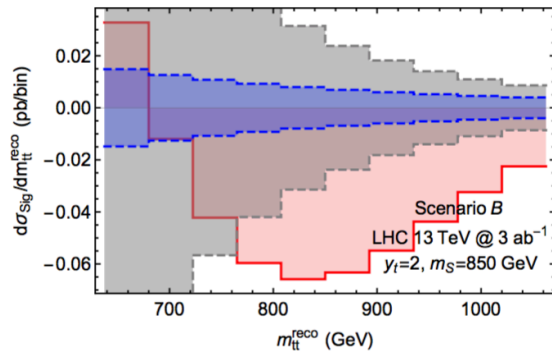
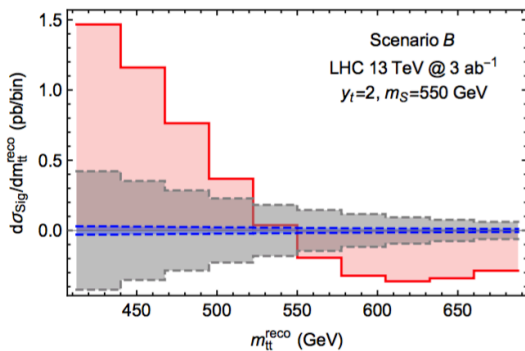
With CPV, new interference between the two heavy nearly degenerate scalars occurs (although the effect might be small) but unique.

# LHC perspectives

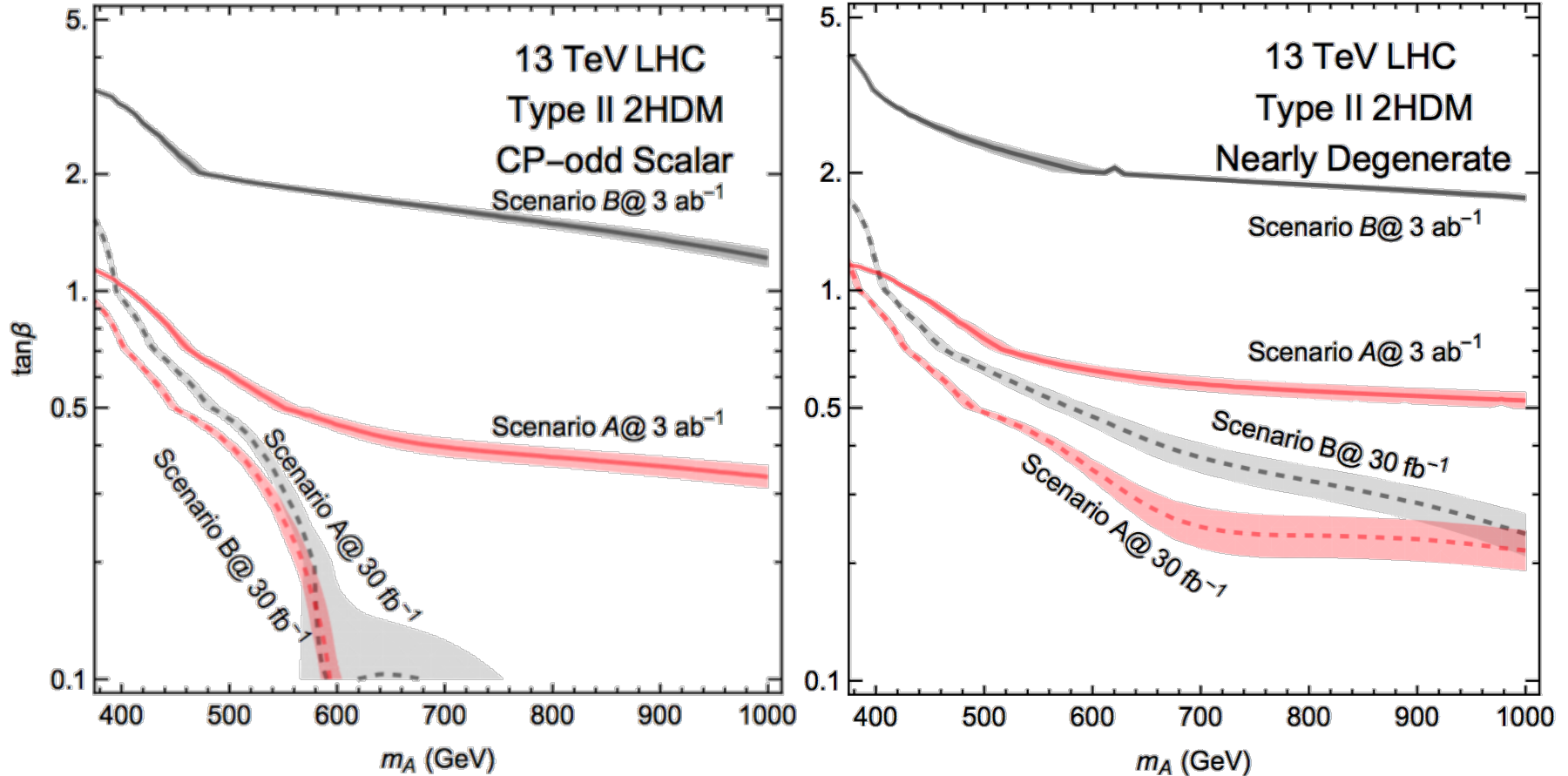
	$\Delta m_{t\bar{t}}$	Efficiency	Systematic Uncertainty
Scenario A	15%	8%	4% at $30 \text{ fb}^{-1}$ , halved at $3 \text{ ab}^{-1}$
Scenario B	8%	5%	4% at $30 \text{ fb}^{-1}$ , scaled with $\sqrt{L}$



Lineshapes for a grid of mass and different Yukawas are generated (because the signal is line-shape and does not scale as simple powers of Yukawa couplings). After smearing, using bins near the scalar mass window, taking both excess and deficits, exclusion potential extracted.



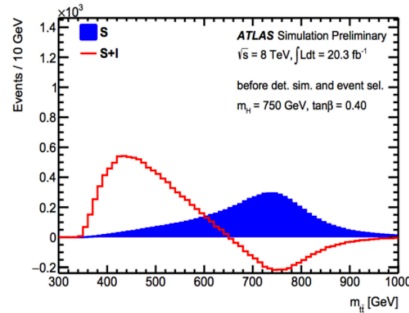
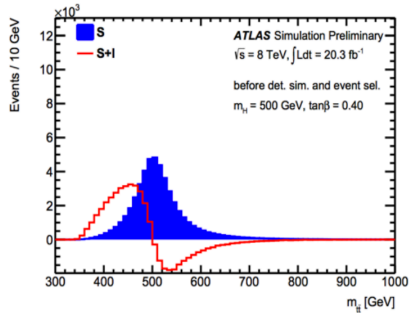
# LHC perspectives—2HDM projections



For the case of nearly degenerate heavy scalars, the physic reach is improved, especially for heavy heavy masses.

## Signal Modeling (A/H → tt̄b̄)

- The signal process is simulated using the generator MadGraph5 v2.0.1 with the Higgs Effective Couplings Form Factor model (implements the production of scalar and pseudoscalar particles through loop-induced gluon fusion)
  - Loop contributions from both bottom and top quarks are taken into account
  - Signal shape is distorted from a simple Breit-Wigner peak, to a peak-dip structure
  - Statistical interpretation of measured event rates in data are compared to the total sum of Signal + Interference + Background (S + I + B)
- The mass of the SM-like Higgs boson, h, is chosen to be 125 GeV and  $\sin(\beta - \alpha)$  is set to 1

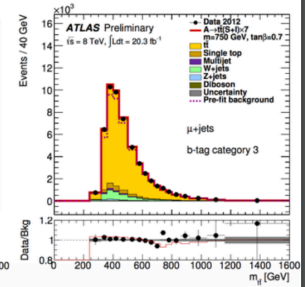
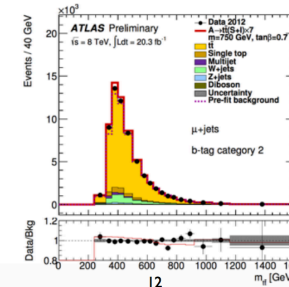
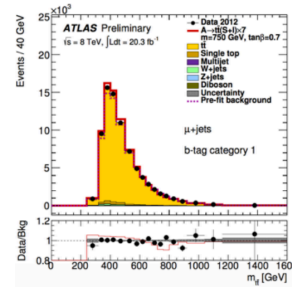


## Event Selection / Mass Reconstruction (A/H → tt̄b̄)

- Analysis targets the tt̄b̄ lepton+jets channel (one W to hadrons one to leptons)
  - Single electron or single muon triggers are used—2 categories (one for e; one for μ)
  - One high p\_T electron or muon; high MET from the escaping neutrino; presence of at least 4 high p\_T jets in the event; at least one jet originating from b quarks must be tagged (70%); Sum of MET and m\_T > 60 GeV (multi-jets suppression)  $m_T^W = \sqrt{2 \cdot p_T^e \cdot E_T^{\text{miss}} \cdot (1 - \cos \phi_{e\nu})}$
- A chi-squared fit is used for assignment of the decay products, then m\_tt is reconstructed
  - Events further classified depending on the b-tagged jet(s) assignment—3 categories

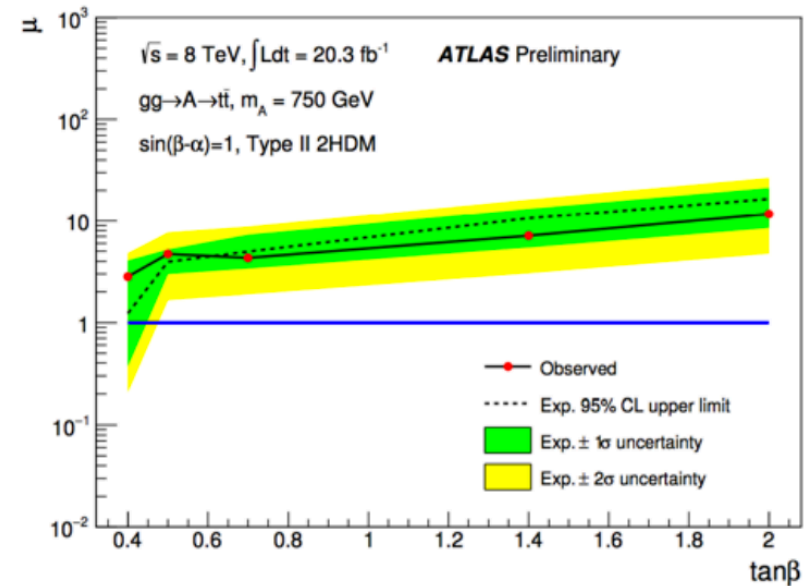
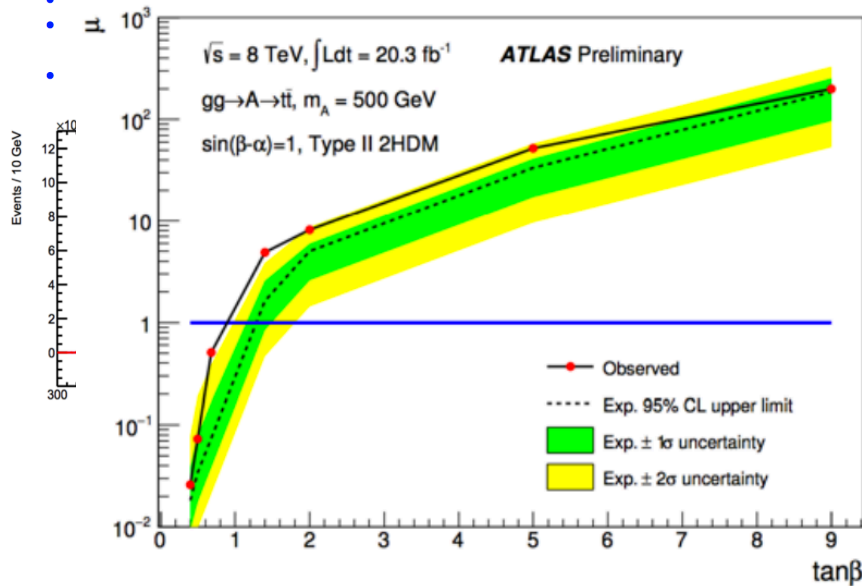
$$\chi^2 = \left[ \frac{m_{jj} - m_W}{\sigma_W} \right]^2 + \left[ \frac{m_{jjb} - m_{jj} - m_{b_h-W}}{\sigma_{b_h-W}} \right]^2 + \left[ \frac{m_{j\ell\nu} - m_{t\ell}}{\sigma_{t\ell}} \right]^2 + \left[ \frac{(p_{T,jj} - p_{T,j\ell\nu}) - (p_{T,b} - p_{T,t\ell})}{\sigma_{\text{diff } p_T}} \right]^2$$

**6 categories in total  
(2 lepton types) x  
(3 b-tagging  
classifications)**



# High-mass Higgs Search Results ( $A/H \rightarrow t\bar{t}b\bar{b}$ )

- No significant excess over Standard Model background expectations is observed
- We set upper limits on the signal strength parameter  $\mu$  as a function of the parameter  $\tan\beta$  for a neutral pseudoscalar  $A$  with a mass of 500 GeV and 750 GeV
- NB: The blue line at  $\mu=1$  corresponds to the signal strength in the Type-II 2HDM



- For a neutral pseudoscalar  $A$ , with a mass of  $m_A = 500 \text{ GeV}$ , parameter values of  $\tan\beta < 0.85$  in the Type-II 2HDM are excluded at the 95% CL. No  $\tan\beta$  values can be excluded for the higher mass point at 750 GeV.

# Summary and outlook

$gg \rightarrow S \rightarrow t\bar{t}$  is a well—motivated channel for the hunt of heavy scalars

The interference effect augmented by the strong phase generated by the top loop generates interesting shapes. **(The effect is always there regardless of the width!)**

Opportunities to increase the observational aspects resides on both the theoretical side (including nearly degenerate bosons, CP phases, additional contributions from light quarks, and heavy colored particles) and experimental side (reducing the systematics with copious tops produced at the LHC, starting to face this challenge by using line-shape profile search ATLAS-2016-073, and move on from there.)

Also see the several later talks in this meeting.

Other channels and effects, including  $t\bar{t}H$ ,  $tH$  (see in N. Craig, F. D’Eramo, P. Drapper, S. Thomas, H. Zhang [arXiv:1504.04630](#) and J. Hajer, Y.-Y. Li, T. Liu J. Shiu [arXiv:1504.07617](#), S. Gori, I.-W. Kim, N. Shah, K. Zurek [arXiv:1602.02782](#), N. Craig, J. Hajer, Y. Li, T. Liu, H. Zhang, [arXiv:1605.08744](#), B. Hespel, F. Maltoni, E. Vryonidou [arXiv:1606.04149](#)),  $H$ +jet, charged Higgs searches, and how stable such effects are against QCD corrections(see a case study in W. Bernreuther, P. Galler, C. Mellein, Z.-G. Si, P. Uwer [arXiv:1511.05584](#)), may have more potentials. Also other decay channels may have such effect large (see in Jung, Sung, Yoon, [arXiv:1510.03450](#), [arXiv:1601.00006](#)).



# Summary and outlook

For scalar mediator DM cases, consequences are:

- Additional decays into DM pairs might change the Branching fractions; but it is not a bad thing (comparing to our conventional wisdom of reducing the signal strength), as we can no longer do zero-width-approximation;
- We need to translate the direct scalar searches into limits on the simplified DM models (as we do for many other DM simplified models);
- All the additional channels we talked about heavy scalar  $t\bar{t}$  searches help:  $t\bar{t}+j$ ,  $t\bar{t}+t+x$ ,  $t\bar{t}+t\bar{t}$ ,  $t\bar{t}+b\bar{b} \rightarrow j+\text{MET}$  (done),  $t+x+\text{MET}$ ,  $t\bar{t}+\text{MET}$ , etc. Or even pair production,  $pp \rightarrow SS \rightarrow t\bar{t}+\text{MET}$ , and no need to worry about interferences.
- All the additional modifications we talked about heavy scalar  $t\bar{t}$  searches apply: bottom-loop, nearly degenerate, CPV effects, heavy vector-like-quark contribution, heavy SUSY particle contribution.

# Backup

$$g_{1,2}^{\tilde{t}}(S) \frac{\sqrt{2}}{v} = \begin{cases} m_t^2 + \cos 2\beta (D_{L/R}^t \sin^2 \theta_{\tilde{t}} + D_{R/L}^t \cos^2 \theta_{\tilde{t}}) \pm \frac{1}{2} m_t X_t \sin 2\theta_{\tilde{t}} & , \text{ for } S = h \\ -\frac{m_t^2}{\tan \beta} - \sin 2\beta (D_{L/R}^t \sin^2 \theta_{\tilde{t}} + D_{R/L}^t \cos^2 \theta_{\tilde{t}}) \mp \frac{1}{2} m_t Y_t \sin 2\theta_{\tilde{t}} & , \text{ for } S = H \\ \mp \frac{1}{2} m_t Y_t \sin 2\theta_{\tilde{t}} & , \text{ for } S = A \end{cases}$$

$$D_L^u = \frac{1}{2} m_W^2 (1 - \frac{1}{3} \tan^2 \theta_W) \cos 2\beta$$

$$D_R^u = \frac{2}{3} m_W^2 \tan^2 \theta_W \cos 2\beta$$

$$D_L^d = -\frac{1}{2} m_W^2 (1 + \frac{1}{3} \tan^2 \theta_W) \cos 2\beta$$

$$D_R^d = -\frac{1}{3} m_W^2 \tan^2 \theta_W \cos 2\beta$$

$$X_t Y_t = \frac{A_t^2}{\tan \beta} - \frac{\mu^2}{\tan \beta} - A_t \mu (1 - \frac{1}{\tan^2 \beta}).$$

$$X_u = A_u - \frac{\mu}{\tan \beta}$$

$$X_d = A_d - \mu \tan \beta$$

$$Y_u = \frac{A_u}{\tan \beta} + \mu$$

$$Y_d = A_b \tan \beta + \mu,$$

zero LR mixing :  $m_{Q_3} = 900 \text{ GeV}, m_{t_R} = 400 \text{ GeV}, X_t = 0$

mh\*<sub>max</sub> :  $m_{Q_3} = 900 \text{ GeV}, m_{t_R} = 540 \text{ GeV}, Y_t = 2X_t = 3415 \text{ GeV}$

$$g_{sgg}(\hat{s}) = \frac{\alpha_s}{2\sqrt{2}\pi} \frac{y_t^s}{m_t} I_{\frac{1}{2}}(\tau_t), \quad \tilde{g}_{sgg}(\hat{s}) = \frac{\alpha_s}{2\sqrt{2}\pi} \frac{\tilde{y}_t^s}{m_t} \tilde{I}_{\frac{1}{2}}(\tau_t), \quad (2.3)$$

where  $I_{\frac{1}{2}}(\tau_t)$  and  $\tilde{I}_{\frac{1}{2}}(\tau_t)$  are the corresponding loop-functions and<sup>1</sup>

$$\tau_t = \frac{\hat{s}}{4m_t^2}, \quad f(\tau) = \begin{cases} -\arcsin^2(\sqrt{\tau}) & \text{for } \tau \leq 1, \\ \frac{1}{4} \left( \log \frac{1+\sqrt{1-1/\tau}}{1-\sqrt{1-1/\tau}} - i\pi \right)^2 & \text{for } \tau > 1 \end{cases}$$

$$I_{1/2}(\tau) = \frac{1}{\tau^2}(\tau + (\tau - 1)f(\tau)), \quad \tilde{I}_{1/2}(\tau) = \frac{f(\tau)}{\tau}. \quad (2.4)$$

$$\mathcal{A}^{\text{even}} \propto y_t g_{sgg} = y_t^2 I_{\frac{1}{2}}(\tau_t), \quad \mathcal{A}^{\text{odd}} \propto \tilde{y}_t \tilde{g}_{sgg} = \tilde{y}_t^2 \tilde{I}_{\frac{1}{2}}(\tau_t). \quad (2.8)$$

We can define the phase of the resonant amplitudes as,

$$\mathcal{A} = \frac{\hat{s}}{\hat{s} - m_S^2 + i\Gamma_S m_S} |\bar{\mathcal{A}}| e^{i\theta_{\bar{\mathcal{A}}}}, \quad \text{with } \theta_{\bar{\mathcal{A}}} \equiv \arg(\bar{\mathcal{A}}). \quad (2.9)$$

$$\hat{\sigma}_{\text{BSM}}^{\text{odd}}(\hat{s}; \tilde{y}_t)(gg \rightarrow S \rightarrow t\bar{t}) = \hat{\sigma}_{\text{B.W.}}^{\text{odd}}(\hat{s}; \tilde{y}_t) + \hat{\sigma}_{\text{Int.}}^{\text{odd}}(\hat{s}; \tilde{y}_t)$$

$$\frac{d\hat{\sigma}_{\text{B.W.}}^{\text{odd}}(\hat{s}; \tilde{y}_t)}{dz} = \frac{3\alpha_s^2 \hat{s}^2}{4096\pi^3 v^2} \beta \left| \frac{\tilde{y}_t^2 \tilde{I}_{\frac{1}{2}}(\tau_t)}{\hat{s} - m_S^2 + im_S \Gamma_S(\hat{s})} \right|^2$$

$$\frac{\hat{\sigma}_{\text{Int.}}^{\text{odd}}(\hat{s}; \tilde{y}_t)}{dz} = -\frac{\alpha_s^2}{64\pi} \frac{\beta}{1 - \beta^2 z^2} \text{Re} \left[ \frac{\tilde{y}_t^2 \tilde{I}_{\frac{1}{2}}(\tau_t)}{\hat{s} - m_S^2 + im_S \Gamma_S(\hat{s})} \right]$$

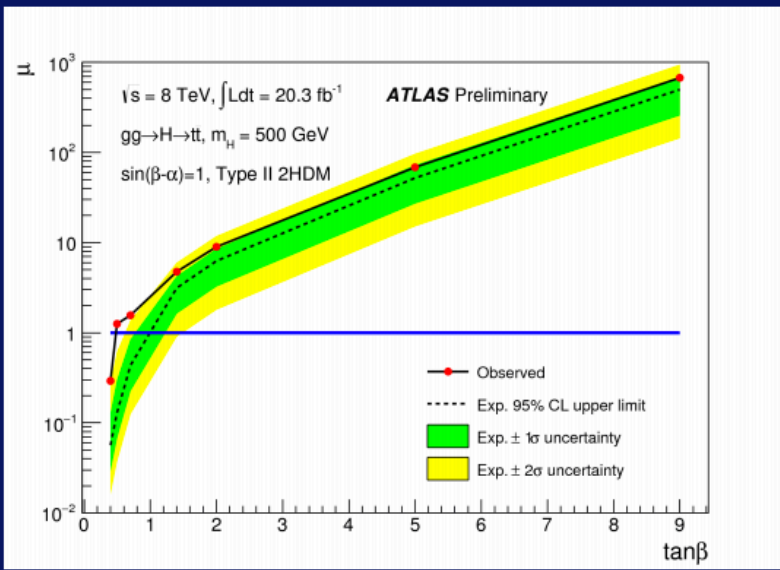
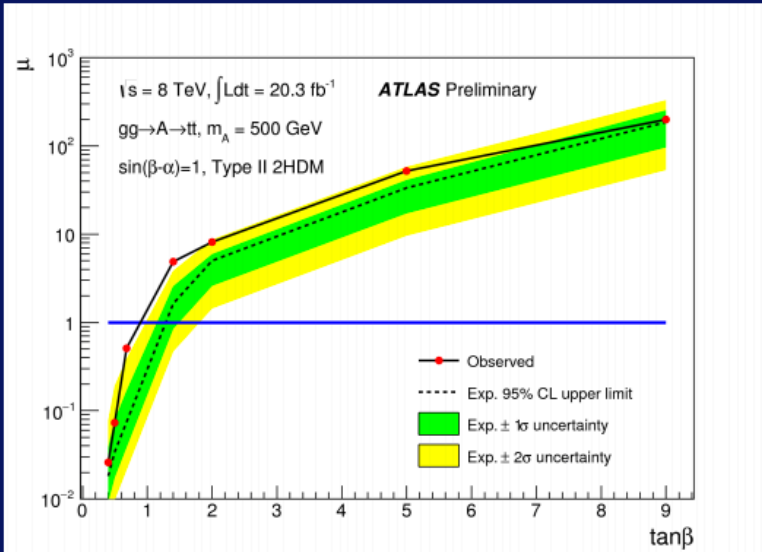
$$\hat{\sigma}_{\text{BSM}}^{\text{even}}(\hat{s}; y_t)(gg \rightarrow S \rightarrow t\bar{t}) = \hat{\sigma}_{\text{B.W.}}^{\text{even}}(\hat{s}; y_t) + \hat{\sigma}_{\text{Int.}}^{\text{even}}(\hat{s}; y_t)$$

$$\frac{d\hat{\sigma}_{\text{B.W.}}^{\text{even}}(\hat{s}; y_t)}{dz} = \frac{3\alpha_s^2 \hat{s}^2}{4096\pi^3 v^2} \beta^3 \left| \frac{y_t^2 I_{\frac{1}{2}}(\tau_t)}{\hat{s} - m_S^2 + im_S \Gamma_S(\hat{s})} \right|^2$$

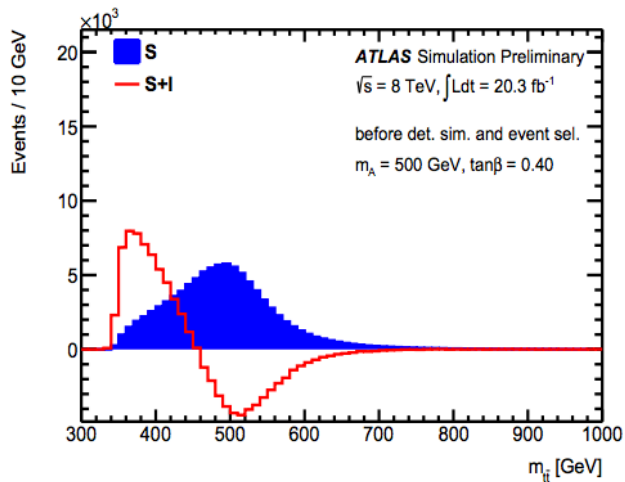
$$\frac{d\hat{\sigma}_{\text{Int.}}^{\text{even}}(\hat{s}; y_t)}{dz} = -\frac{\alpha_s^2}{64\pi} \frac{\beta^3}{1 - \beta^2 z^2} \text{Re} \left[ \frac{y_t^2 I_{\frac{1}{2}}(\tau_t)}{\hat{s} - m_S^2 + im_S \Gamma_S(\hat{s})} \right]$$

$$\frac{d\sigma_{\text{Int.}}^{S_1-S_2}(\hat{s})(gg \rightarrow S_1, S_2 \rightarrow t\bar{t})}{dz} = \frac{3\alpha_s^2 \hat{s}^2}{2048\pi^3 v^2} \text{Re} \left[ \frac{(y_{t,S_1} y_{t,S_2} |I_{\frac{1}{2}}(\tau_t)|^2 + \tilde{y}_{t,S_1} \tilde{y}_{t,S_2} |\tilde{I}_{\frac{1}{2}}(\tau_t)|^2) (\beta^2 y_{t,S_1} y_{t,S_2} + \tilde{y}_{t,S_1} \tilde{y}_{t,S_2})}{(\hat{s} - m_{S_1}^2 + im_{S_1} \Gamma_{S_1}(\hat{s})) (\hat{s} - m_{S_2}^2 - im_{S_2} \Gamma_{S_2}(\hat{s}))} \right] \quad (6)$$

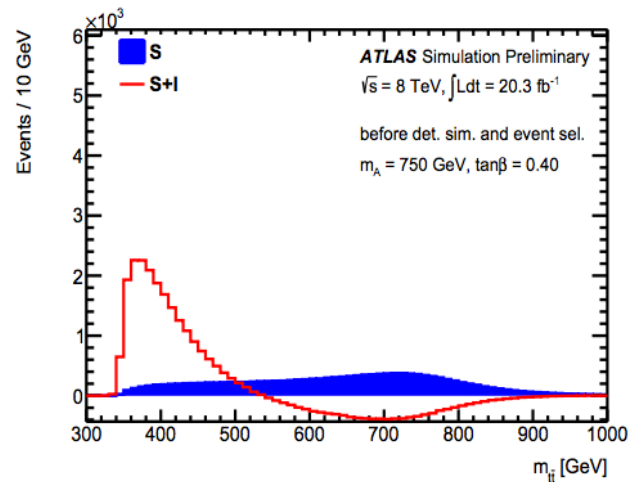
# First interference studies at ATLAS



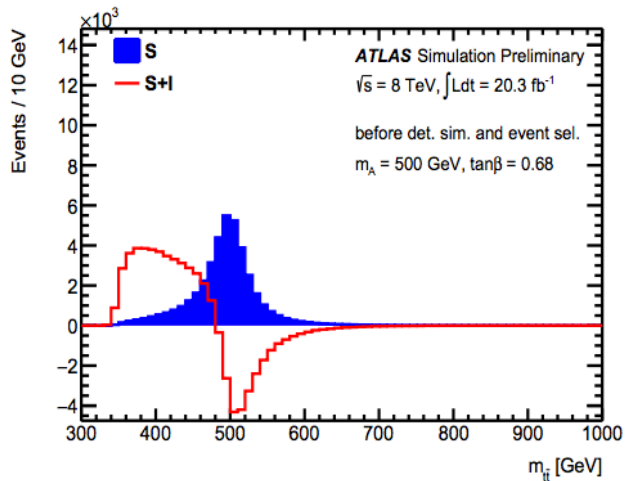
ATLAS-2016-073



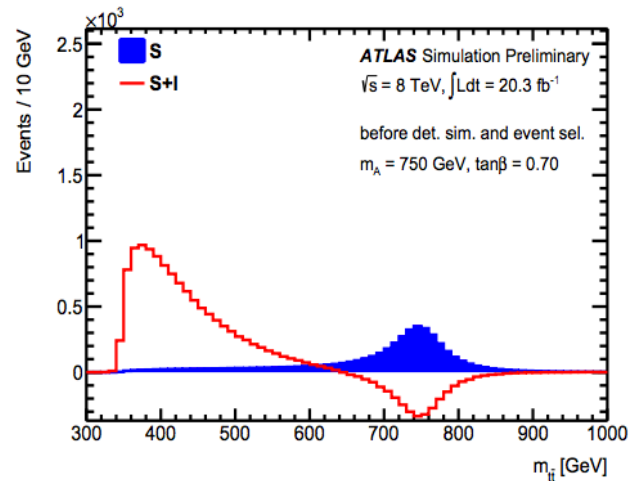
(a)  $m_A = 500$  GeV,  $\tan \beta = 0.40$



(b)  $m_A = 750$  GeV,  $\tan \beta = 0.40$



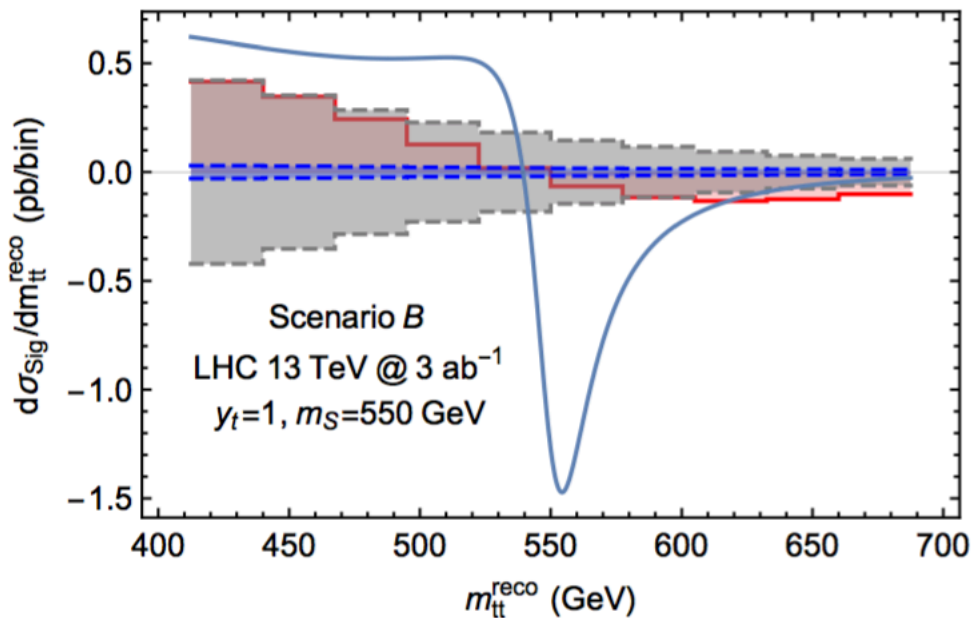
(c)  $m_A = 500$  GeV,  $\tan \beta = 0.68$



(d)  $m_A = 750$  GeV,  $\tan \beta = 0.70$

# LHC perspectives

	$\Delta m_{t\bar{t}}$	Efficiency	Systematic Uncertainty
Scenario A	15%	8%	4% at 30 fb <sup>-1</sup> , halved at 3 ab <sup>-1</sup>
Scenario B	8%	5%	4% at 30 fb <sup>-1</sup> , scaled with $\sqrt{L}$



Blue curve, the signal lineshape before smearing;

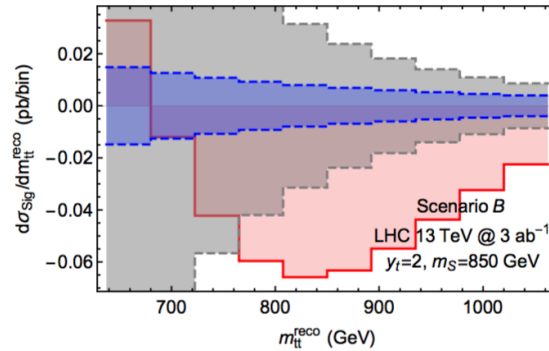
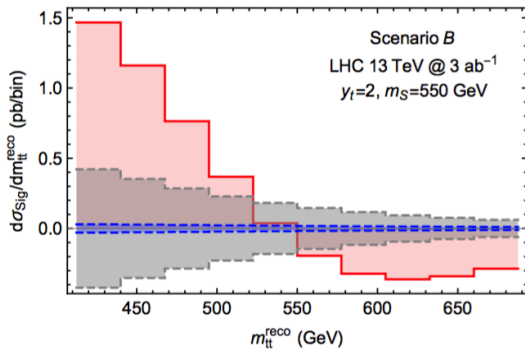
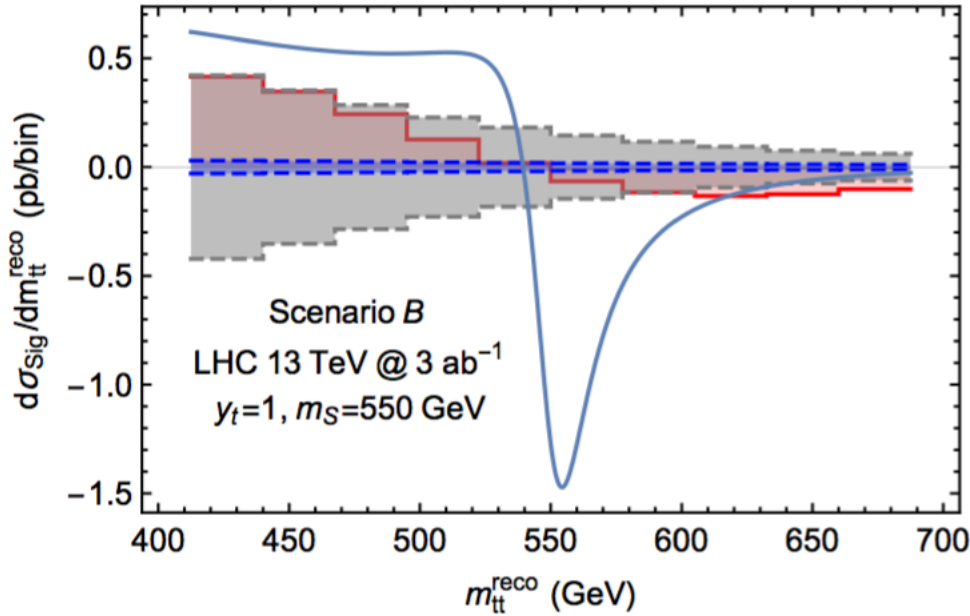
Red Histogram, the signal after smearing and binning;

Gray and blue histograms, the total and statistical uncertainties;



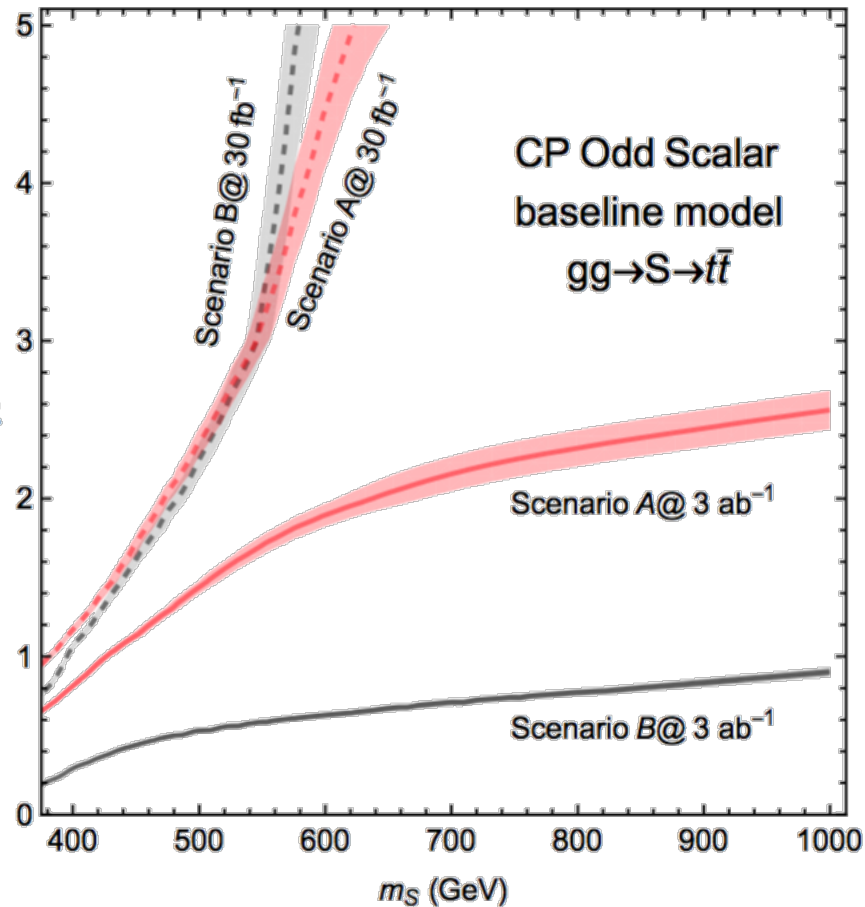
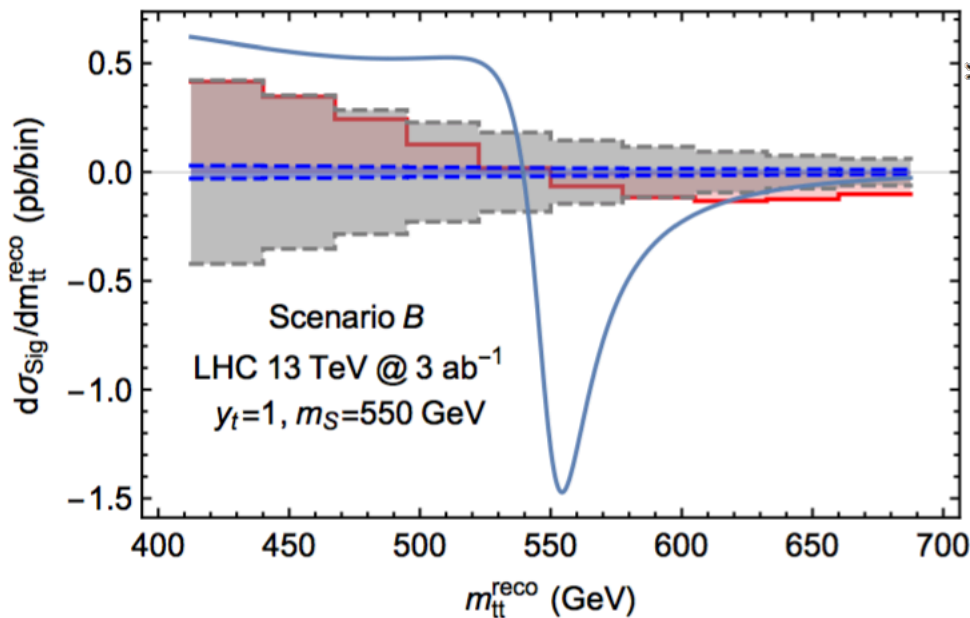
# LHC perspectives

	$\Delta m_{t\bar{t}}$	Efficiency	Systematic Uncertainty
Scenario A	15%	8%	4% at 30 fb <sup>-1</sup> , halved at 3 ab <sup>-1</sup>
Scenario B	8%	5%	4% at 30 fb <sup>-1</sup> , scaled with $\sqrt{L}$

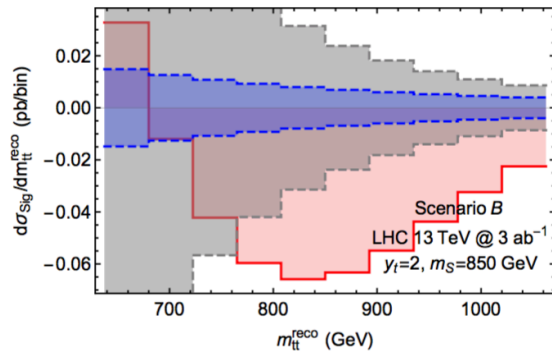
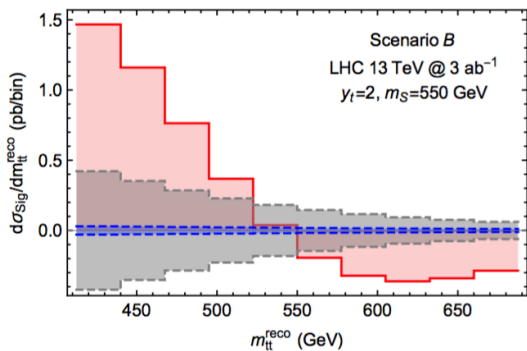


# LHC perspectives

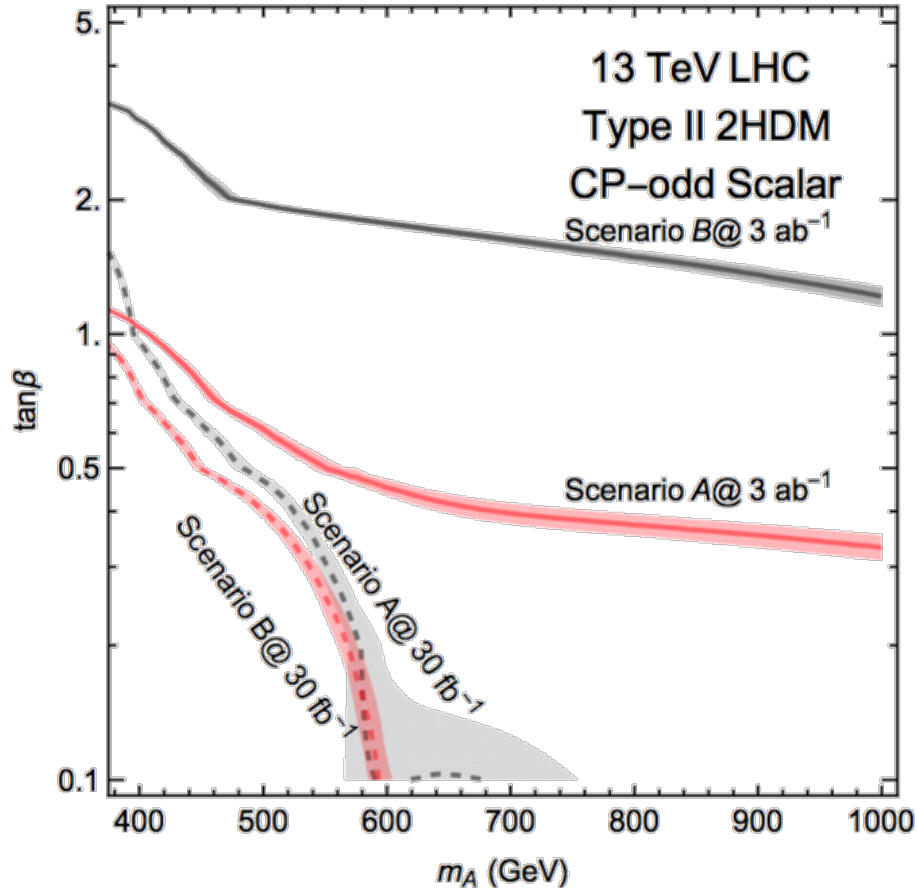
	$\Delta m_{t\bar{t}}$	Efficiency	Systematic Uncertainty
Scenario A	15%	8%	4% at $30 \text{ fb}^{-1}$ , halved at $3 \text{ ab}^{-1}$
Scenario B	8%	5%	4% at $30 \text{ fb}^{-1}$ , scaled with $\sqrt{L}$



Lineshapes for a grid of mass and different Yukawas are generated (because the signal is line-shape and does not scale as simple powers of Yukawa couplings). After smearing, using bins near the scalar mass window, taking both excess and deficits, exclusion potential extracted.



# LHC perspectives—2HDM projections



For a Type II 2HDM, the bottom quark effects are mainly in modifying the production vertex and provide some decay branching fraction suppression; Regions below the curves are excluded; In general can only cover the very low  $\tan\beta$  regime, optimistic LHC performance scenario B could cover up to  $\tan\beta$  around 1~2 up to 1 TeV.